EFFECTS OF CARNALLITE CONTENT ON EXTRACTION RATIO AND BOREHOLE STABILITY OF POTASH MINES

Amornrat Luangthip, Supattra Khamrat, and Kittitep Fuenkajorn*

Received: September 05, 2016; Revised: December 13, 2016; Accepted: December 13, 2016

Abstract

The mechanical properties of rock salt with various amounts of carnallite content are determined in the laboratory. The compressive and tensile strengths and elastic moduli of the specimens decrease exponentially with the increasing carnallite content ($C_{\%}$). The Poisson's ratios increase linearly from 0.27 for pure halite to 0.39 for pure carnallite. The effects of the carnallite content tend to act equally throughout the range of the confining pressures used here (0-12 MPa). The Hoek-Brown strength criterion fits well with the strength results under the various amounts of $C_{\%}$, and can be applied to determine the appropriate extraction ratio and stability of exploratory boreholes. When the $C_{\%}$ increases, the pillar strength and extraction ratio decrease, but the excavated rock contains a higher concentration of sylvite (KCl). Conversely, for the lower $C_{\%}$ the pillar strength and extraction ratio are higher, but the extracted rock contains a lower concentration of KCl. The dilation and failure zones around the exploratory boreholes increases with the depth and carnallite content.

Keywords: Elastic modulus, strength, sylvite, rock salt

Introduction

The rapid growth of the exploitation of resources and the potential development of underground space utilization have called for a true understanding of the mechanical behavior of the Maha Sarakham rock salt, particularly that of the Middle and Lower Salt members. One distinct implication is that the mechanical properties of Maha Sarakham salt tend to have high variations. These variations may be caused by internal (intrinsic) factors (i.e., differences in grain sizes, carnallite content, and cohesive forces between the grains), and by external factors (differences in specimen sizes, loading rates, stress-paths, and testing temperatures). These uncertainties have raised a question about the representativeness and

Geomechanics Research Unit, Institute of Engineering, Suranaree University of Technology, Nakhon Ratchasima 30000, Thailand. E-mail: kittitep@sut.ac.th
* *Corresponding author*

reliability of laboratory-determined properties when applied to the design and analyses of engineering structures in the salt mass.

Inclusions and impurities in salt can affect its creep deformation and strength. The degree of impurity is different for different scales. Handin *et al*. (1984) stated that natural rock salt may contain 3 forms of impurities: (1) extraneous minerals may be disseminated between halite grains, (2) some water may be trapped in the halite crystal structure or it may appear in brine-filled fluid inclusions or along grain boundaries, and (3) foreign ions such as K^+, Ca^{2+}, Mg^{2+}, Br^-, and I^- may be embedded in the crystal structure. The coupled effects of the impurities on the mechanical properties of salt can be very complicated (Franssen and Spiers, 1990; Raj and Pharr, 1992; Senseny *et al*., 1992). Fuenkajorn *et al*. (2011) conducted mechanical testing on the Middle Salt member and found that the compressive and tensile strengths of the rock increase with the increasing anhydrite content. Handin *et al*. (1984) compared the steady-state flow parameters obtained for pure halite with those for salt samples with 0.6% $MgCl_2$ inclusions and with 0.1% KCl inclusions, and concluded that the inclusions appreciably increase the creep rate of salt.

Potash has become 1 of the prominent ores associated with Maha Sarakham salt. In the Sakon Nakhon basin, Asia Pacific Potash Corporation (APPC) has carried out an extensive exploration programme, and drawn a detailed mine plan for extracting sylvite from the upper portion of the Lower Salt member (Crosby, 2005). It has been estimated that the inferred reserves of sylvite are about 302×10^9 t for the Udon South deposit and 665×10^9 t for the Udon North deposit. In the Khorat basin, Asean Potash Mining Company has also conducted extensive studies and developed exploratory inclined shafts to investigate the feasibility of extracting carnallite from the Lower Salt member.

Extensive laboratory testing has been performed to determine the mechanical and rheological properties and behavior of the Maha Sarakham rock salt under a variety of boundary and loading conditions. Wisetsaen *et al*. (2015) suggested that the tensile elastic modulus of the salt linearly decreases with an increasing temperature. The salt specimens also exhibit time-dependent behavior under tension, particularly under high temperatures and low loading rates. Fuenkajorn *et al*. (2012) concluded from their experimental results that the salt's elasticity and compressive strength increase with the loading rates. The strains induced at failure decrease as the loading rate increases. Sriapai *et al*. (2013) found that the intermediate principal stress (σ_2) or Lode parameter can affect the compressive strengths of the Maha Sarakham salt. The salt's elasticity, however, tends to be independent of σ_2. The above-mentioned research concentrated on the properties and behavior of rock salt with virtually pure halite. The effects of the carnallite content on the rock's mechanical properties have never been addressed and investigated. Such knowledge is important for carnallite ore exploitation and excavation design in the basins.

The objectives of this study are to determine the effects of the carnallite content on the strength and elasticity of the rock salt, to calculate the appropriate extraction ratios of the potash mines while maintaining sufficient stability of the support pillars, and to predict the mechanical stability of exploratory boreholes at the mine's horizon. The effort involves performing characterization testing of the rock salt specimens with various amounts of carnallite content and the derivation of strength criterion to describe the rock's strengths and deformability as affected by the carnallite. The results are applied to determine the pillar and borehole stability in potash mines.

Sample Preparation

Rock salt blocks ($0.5\times0.5\times0.7$ m^3) were collected from an underground carnallite mine in the northeast of Thailand. They came from the Lower Salt member of the Maha Sarakham formation. The carnallite beds are commonly found near the top of the Lower Salt member. Hite and Japakasetr (1979), Hite (1982), and Suwanich (1983) stated that the carnallite's origin should be a primary mineral and that it is often found near flanks or shelves of salt domes or anticlines. Only rock salt blocks that contain halite and carnallite are used to prepare the specimens in this study. The carnallite

appears as crystalline or granular masses. In some blocks the interbeddings of carnallite and halite can be clearly seen. In some blocks the contacts between the 2 minerals cannot be defined. An attempt was made here to obtain rock cores by using an impregnated diamond coring bit with a 54 mm diameter. During drilling, the specimens with a high carnallite content tended to break along the bedding planes. The obtained core length was less than twice the core diameter. The specimens used for the uniaxial and triaxial compression tests, and the uniaxial and triaxial creep tests are therefore prepared as rectangular blocks with nominal dimensions of 54×54×108 mm^3. Figure 1 shows some examples of the rectangular block specimens. For the Brazilian tension test, 62-mm diameter disks can be prepared with a thickness-to-diameter ratio of 0.5.

Chemical analyses by X-ray diffraction (XRD) performed on some specimens show that the primary mineral compositions of the specimens are halite and carnallite, which are of interest in this study (Table 1). The halite crystals are about 2-5 mm. The size of the carnallite crystals varies greatly from 1 mm to 2 cm. Other minerals are relatively small and tend to appear in about the same amounts in all specimens. Due to the difference of the densities between halite and carnallite, the carnallite content ($C_{\%}$) for each specimen can be estimated by:

$$C_{\%} = \left(\frac{\rho_s - \rho}{\rho_s - \rho_c} \right) \times 100 \quad (1)$$

where ρ is the specimen density, ρ_s is the density of halite (2.16 g/cc), and ρ_c is the density of carnallite (1.60 g/cc) (Klein *et al.*, 1998).

Tension Test

The Brazilian tension test method and calculation follow the ASTM (D3967) standard practice

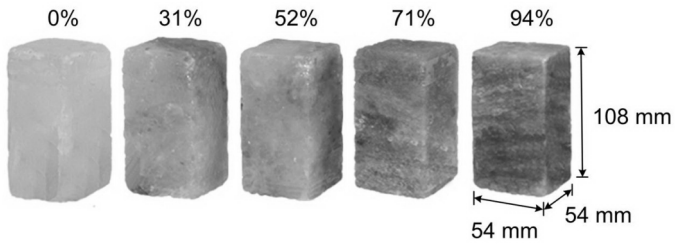

Figure 1. Some block specimens prepared for uniaxial and triaxial compression tests

Table 1. Chemical compositions of some specimens

Components	Sample no. 1	Sample no. 2	Sample no. 3	Sample no. 4
Carnallite ($KMgCl_3$ $6H_2O$)	0.05	24.75	38.31	52.98
Halite (NaCl)	92.40	64.60	42.80	35.97
$MgCl_2$	5.71	8.93	9.69	5.55
Calcite ($CaCO_3$)	0	0.21	0.48	1.92
Anhydrite ($CaSO_4$)	0.11	0.17	0.65	1.23
Sylvite (KCl)	0.09	0.19	6.10	1.01
Hydrophilite ($CaCl_2$)	0	0	1.64	0.56
Wuestite	0	0.06	0.43	0.44
Calcium Chloride (CaCl)	1.65	1.08	0.89	0.33
Density (g/cc)	2.11	1.96	1.89	1.76
$C_{\%}$ (determined by density ratio)	8.56	36.12	49.01	71.08

(ASTM, 1998) and the ISRM suggested methods (Brown, 1981). Over 60 specimens with various amounts of carnallite content have been tested. The specimens have nominal diameters of 62 mm with a length-to-diameter ratio of 0.5. The bedding planes are parallel to the specimen axis. Figure 2 plots the Brazilian tensile strengths (σ_B) as a function of the $C_{\%}$ varying from 0% (pure halite) to 94%. Post-test observations show that there are 2 combined modes of fracturing in the specimens: cleavage fracturing in the halite and conchoidal fracturing in the carnallite. The tensile strengths decrease exponentially with the increasing carnallite content:

$$\sigma_B = 1.660 \cdot \exp\left(-0.020 \cdot C_{\%}\right) \; C \text{ MPa} \qquad (2)$$

The tensile strengths for pure carnallite specimens are about 14% of those for pure halite specimens. The strengths show relatively high intrinsic variability ($R^2 = 0.873$) for all the $C_{\%}$. This could be explained by the fact that the tensile splitting of the disk specimen may be governed by the orientations and amounts of halite and carnallite along the loading diameters. Under the same $C_{\%}$, the specimens may show high strengths if the tensile splitting occurs through the salt crystals. The low strengths may be obtained for the tensile cracks that are largely induced through the carnallite crystals.

Compression Test

A polyaxial load frame (Fuenkajorn *et al.*, 2012) has been used to apply lateral and axial stresses on the rectangular specimens. Sixty specimens have been tested. Except for the specimen geometry, the test procedure and calculations follow the ASTM (D7012-07) standard practice (ASTM, 2007).

The uniaxial compressive strengths (σ_c) as a function of the $C_{\%}$ at dilation and at failure are shown in Figure 3. The dilation strength is the point at which the specimen is loaded and deformed to its elastic limit. Beyond this point the micro-cracks are initiated, the specimen volume increases, and the axial stress-strain relationship is no longer linear. The results show that the strengths at dilation ($\sigma_{c,d}$) and at failure ($\sigma_{c,f}$) exponentially decrease with the increasing $C_{\%}$, and can be represented by:

$$\sigma_{c,f} = 8.89 \cdot \exp\left(-0.021 \cdot C_{\%}\right) \text{ MPa} \qquad (3)$$

$$\sigma_{c,f} = 23.19 \cdot \exp\left(-0.012 \cdot C_{\%}\right) \text{ MPa} \qquad (4)$$

The exponential equations above fit relatively well with the strength results ($R^2 > 0.8$). The dilation strength is about 40% of the failure strength for the rock salt specimens with pure halite ($C_{\%} = 0$), and about 10% of the failure strength for the specimens with over 80% carnallite content. Shear fractures are induced in all specimens. They cut through both the halite and carnallite crystals. No distinctive difference in the failure mode is found among specimens with a different $C_{\%}$.

For the triaxial compression testing, the constant and uniform lateral stresses ($\sigma_2 = \sigma_3$) range from 1.7, 3, 5, 7, and 9 to 12 MPa. The specimen deformations are monitored along the 3 loading directions and are used to calculate

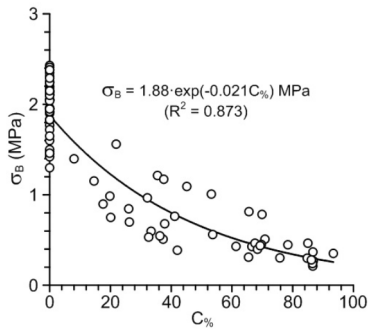

Figure 2. Brazilian tensile strength as a function of the carnallite content

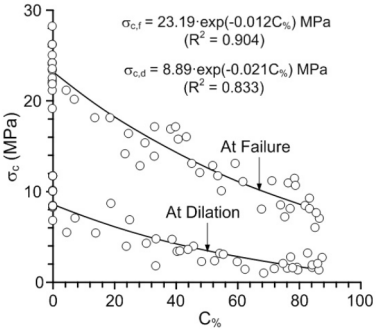

Figure 3. Uniaxial compressive strengths as a function of the carnallite content

the principal strains during loading. Post-test specimens from the triaxial testing show 2 types of failure mode: extensile splitting and compressive shear failure (Figure 4). The rock salt specimens with various percentages of carnallite failed mainly under the shear fractures and extensile splitting mode, particularly under low confining stresses. Shear fractures are found in the specimens that failed under high confining stresses. Figure 5 shows the stress-strain curves monitored from the triaxial test specimens with various amounts of carnallite content and confining pressures. The effect of the carnallite can be observed by the reduction of the failure stresses and the increase of the failure strains, particularly under low confining pressures. All post-test specimens show multiple shear failures.

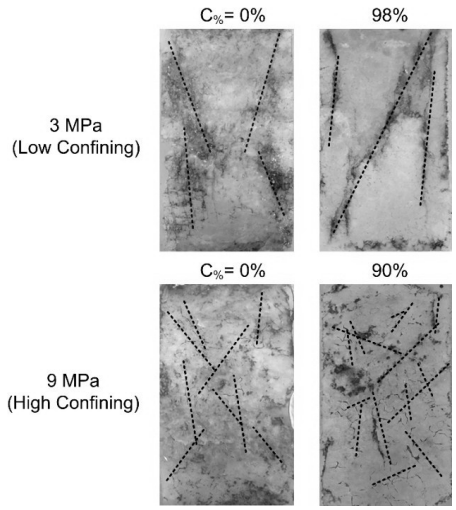

Figure 4. Some post-test specimens showing the combination of shear and extensile failures

The elastic modulus (E) and Poisson's ratio (ν) of the specimens are determined from the tangent of the stress-strain curves at 40% of the failure stress. On the assumption that the specimens are isotropic, the shear (rigidity) modulus (G), Lamé constant (λ), and Poisson's ratio (ν) can be calculated from the following relations (Jaeger *et al*., 2007):

$$\tau_{\text{oct}} = (1/3)\left[(\sigma_1 - \sigma_2)^2 + (\sigma_2 - \sigma_3)^2 + (\sigma_3 - \sigma_1)^2\right]^{1/2} \quad (5)$$

$$\gamma_{\text{oct}} = (1/3)\left[(\varepsilon_1 - \varepsilon_2)^2 + (\varepsilon_2 - \varepsilon_3)^2 + (\varepsilon_3 - \varepsilon_1)^2\right]^{1/2} \quad (6)$$

$$G = (1/2)(\tau_{oct}/\gamma_{oct}) \quad (7)$$

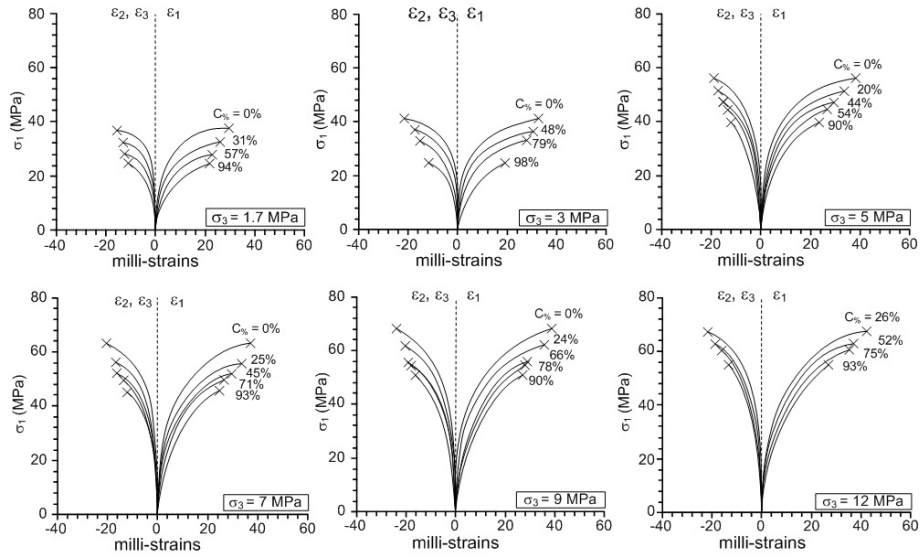

Figure 5. Stress-strain curves obtained from the triaxial compression test for various confining pressures

Table 2. Principal stresses at dilation and at failure and elastic parameters

$\sigma 3$ (MPa)	$C_{\%}$	$\sigma 1,d$ (MPa)	$\sigma 1,f$ (MPa)	G (GPa)	λ (GPa)	ν	E (GPa)
0	0	11.3	23.4	8.47	5.58	0.29	21.8
	19	9.6	20.8	5.49	3.14	0.28	13.3
	25	8.4	12.3	3.28	2.62	0.28	8.4
	45	5.3	9.9	2.23	2.15	0.31	6.5
	87	3.1	6.7	1.09	1.17	0.39	2.6
1.7	0	24.0	37.6	8.27	6.01	0.27	20.0
	31	18.7	32.5	2.89	2.40	0.29	9.9
	57	16.3	28.1	2.03	1.87	0.33	5.1
	94	13.5	25.0	1.33	1.04	0.35	3.3
3	0	28.5	41.9	7.78	7.86	0.27	16.6
	0	24.7	45.1	7.03	6.40	0.26	15.8
	48	24.1	36.9	1.85	5.27	0.32	6.1
	79	17.5	32.8	1.67	1.63	0.34	4.4
5	0	32.1	56.0	8.02	14.99	0.27	17.1
	0	36.9	54.1	9.52	11.30	0.27	16.9
	20	31.6	51.9	3.62	4.15	0.30	10.5
	44	28.6	47.4	2.13	3.41	0.31	8.6
	54	25.7	45.1	2.02	1.90	0.33	5.7
	94	21.7	39.7	0.90	1.60	0.40	2.4
7	0	38.4	60.0	7.01	15.30	0.26	16.5
	0	42.3	63.6	10.10	13.80	0.26	16.1
	25	36.4	56.1	3.91	6.19	0.28	9.9
	45	24.3	52.7	2.42	3.44	0.31	7.0
	71	31.7	50.4	1.45	2.73	0.35	4.2
	93	26.5	46.0	0.85	1.92	0.38	3.0
9	0	42.6	67.0	7.49	14.57	0.27	16.1
	0	47.0	71.1	6.62	15.48	0.26	16.3
	24	41.0	60.8	3.95	9.03	0.29	10.2
	66	33.4	54.7	1.58	3.08	0.35	5.3
	78	31.0	53.0	1.03	2.36	0.37	4.2
	90	27.8	50.2	0.82	2.18	0.40	2.9
12	0	51.0	81.2	10.90	4.57	0.26	16.9
	26	45.6	68.1	4.15	7.27	0.30	10.8
	52	39.3	63.6	2.40	4.99	0.34	7.7
	75	35.3	61.4	1.22	2.99	0.38	4.8
	93	30.1	55.8	0.74	2.63	0.40	3.5

$$3\sigma_m = (3\lambda + 2G)\varepsilon_v \quad (8)$$

$$\nu = \lambda/(2\lambda + G) \quad (9)$$

where τ_{oct}, γ_{oct}, σ_m, and ε_v are the octahedral shear stress, the octahedral shear strain, mean stress, and volumetric strain at dilation (the point where the elastic parameters are determined). Table 2 gives the calculated elastic parameters for each specimen. The elastic modulus rapidly decreases with the increasing $C_{\%}$ (Figure 6(a)):

$$E = 16.81 \cdot \exp(-0.021 \cdot C_{\%}) \text{ GPa} \quad (10)$$

The elastic moduli of the pure halite specimens are about 17-22 GPa, which agrees with those obtained by Sriapai *et al*. (2013) and Funkajorn *et al*. (2012). Extrapolation of the above equation suggests that the pure carnallite specimens would have the elastic moduli of less than 2 GPa. The increases of the Poisson's ratio with the increasing carnallite content can be represented by a linear equation (Figure 6(b)):

$$\nu = 0.002 \cdot C_{\%} + 0.264 \quad (13)$$

The results suggest that under loading the carnallite tends to dilate more than the halite. This is probably because carnallite is softer and has no cleavage while the stronger halite crystal has 3 mutually perpendicular cleavage planes.

Strength Criterion

The Hoek-Brown criterion (Hoek and Brown, 1980) is used here to describe the relationship between the major (σ_1) and minor (σ_3) principal stresses at dilation and at failure of the triaxial test results:

$$\sigma_1 = \sigma_3 + \left(m\sigma_c\sigma_3 + s\sigma_c^2\right)^{1/2} \quad (14)$$

where m and s are material constants. For intact rock, $s = 1$. The parameter m varies from less than 1 for soft rocks to greater than 1000 for strong rocks (Hoek and Brown, 1980).

The criterion can be rewritten as a function of the principal stresses at dilation and at failure:

$$\sigma_{1,d} = \sigma_3 + \left(m_d \cdot \sigma_3 \cdot \sigma_{c,d} + s\sigma_{c,d}^{\ 2}\right)^{1/2} \quad (15)$$

$$\sigma_{1,f} = \sigma_3 + \left(m_f \cdot \sigma_3 \cdot \sigma_{c,f} + s\sigma_{c,f}^{\ 2}\right)^{1/2} \quad (16)$$

where m_d and m_f represent the conditions at dilation and at failure. Via regression analysis, they can be defined as a function of the $C_{\%}$ as:

$$m_d = -0.085 \cdot C_{\%} + 14.73 \quad (17)$$

$$m_f = -0.033 \cdot C_{\%} + 18.09 \quad (18)$$

By substituting Equations (3), (4), (17), and (18) into Equations (15) and (16), the complete failure and dilation criteria for

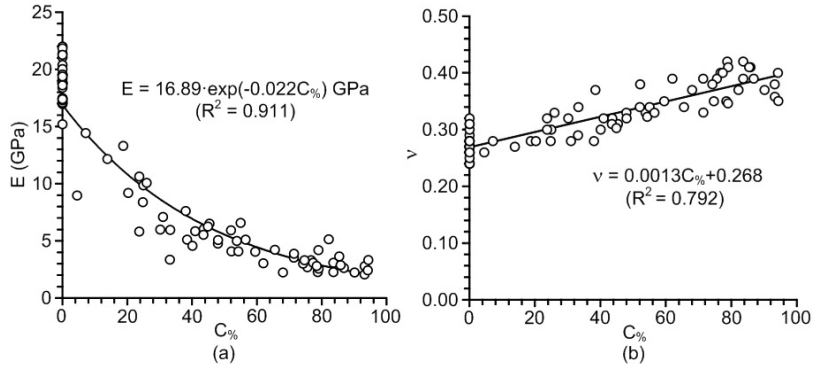

Figure 6. Elastic modulus (a) and Poisson's ratio (b) as a function of the carnallite content

specimens with varied $C_{\%}$ can be obtained. Figure 7 compares the criterion with the strength data. The criterion fits well with the strength data ($R^2 > 0.9$). The parameter m decreases with the increasing $C_{\%}$. The effects of carnallite on the triaxial compressive strengths become smaller as the confining pressure increases.

The strength data can also be presented in an alternative form to describe the rock's strengths as affected by the $C_{\%}$ under multiaxial stress states. Figure 8 shows the strength diagrams with the $C_{\%}$ values where their locations indicate the corresponding magnitudes of the mean stress and the octahedral shear strengths at dilation ($\tau_{oct,d}$) and at failure ($\tau_{oct,f}$). Interpolation between these $C_{\%}$ points allows derivation of the $\tau_{oct,d}$ and $\tau_{oct,f}$ as a function of σ_m under the selected magnitudes of the carnallite content, which can be represented by a set of power equations:

$$\tau_{oct,d} = \left(-0.0089 \cdot C_{\%} + 3.26\right) \cdot \sigma_m^{-0.0008 \cdot C_{\%} + 0.55} \quad (19)$$

$$\tau_{oct,f} = \left(-0.016 \cdot C_{\%} + 3.50\right) \cdot \sigma_m^{-0.0014 \cdot C_{\%} + 0.63} \quad (20)$$

These equations can be used to determine the rock's strengths under the multiaxial stress condition (to be described in the following sections).

Pillar Stability

The tributary area concept is applied here to determine the extraction ratio of the mine's horizon at different depths (100 m - 200 m). To describe the extraction ratio in terms of pillar

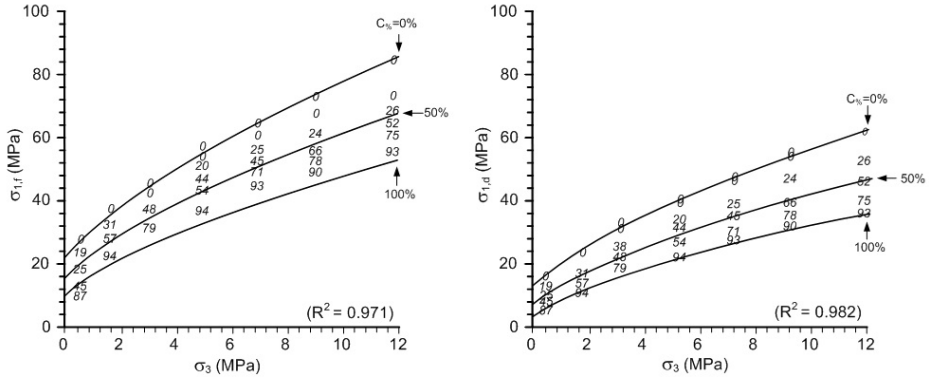

Figure 7. Major principal stress at dilation (a) and at failure (b) as a function of the confining pressure

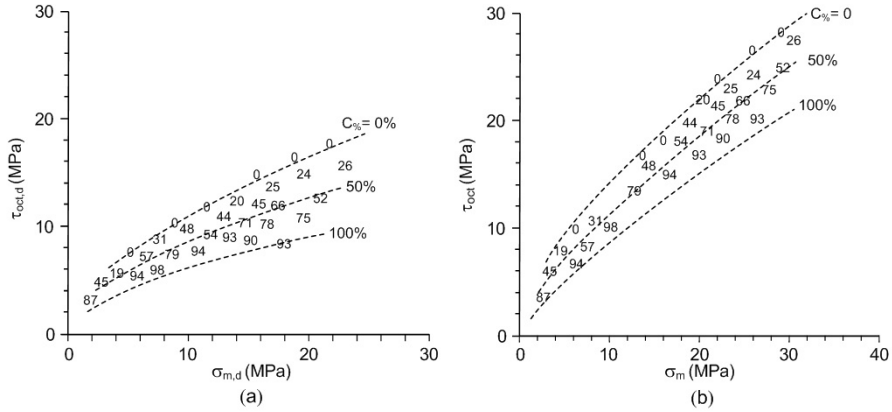

Figure 8. Octahedral shear strength (τ_{oct}) at dilation (a) and at failure (b) as a function of the mean stress (σ_m) for various confining pressures (σ_3) and the carnallite content

stress, the expression obtained by Biron and Arioglu (1980) can be used:

$$e = 1 - \left[(\gamma \cdot H) / \sigma_P \right] \times 100 \qquad (21)$$

where e is the extraction ratio, H is the depth of cover, γ is the average rock unit weight, and σ_P is the pillar stress. Figure 9 shows the extraction ratios at dilation and failure which decrease with the increasing $C_{\%}$ and depth.

The pillar stress can be calculated from the compressive strength of the rock with an appropriate factor of safety (FS),

$$\sigma_P = \sigma_c / \mathrm{FS} \qquad (22)$$

where (σ_c) represents the dilation or failure for the varying carnallite content. The extraction ratio therefore depends on the strength of the rock salt, depth and FS. Based on the chemical compositions, the carnallite contains 26.8% by weight of sylvite (KCl) which is of interest here. At 100, 150, and 200 m depths, and for the FS of 1.1 the amount of KCl is related to the extraction ratio as:

$$\mathrm{KCl} = \left[(26.8 \cdot C_{\%}) / 100 \right] \times e \qquad (23)$$

Figure 10 shows the weight percent of sylvite (KCl) as a function of the $C_{\%}$ for various depths under the FS = 1.1. The amount of KCl that can be extracted initially increases with the $C_{\%}$ until an optimum value is reached. Then the extracted KCl decreases under the large amount of the $C_{\%}$. The lower depths show lower amounts of extracted KCl. The diagrams in Figure 10 can be used to make an initial plan for the potash mines while considering the amount of carnallite, depth, and FS. For example, at 100, 150, and 200 m depths the optimum amounts of extracted sylvite would be about 15%, 10%, and 7% where they are equivalent to the percentages of carnallite of 100%, 75%, and 65%, respectively. They should be mined with the extraction ratios of 60%, 45-55%, and 35-45%, respectively.

Borehole Stability

The strength criterion derived earlier is applied to determine the stability of the rock salt around a borehole subjected to uniform external and internal pressures. This is primarily to demonstrate the potential application of the strength criterion that has been derived from test data under the different $C_{\%}$ values.

The stress distributions around a circular borehole can be calculated under the plane strain condition by using the Kirsch solution (Brady and Brown, 1985). The radial (σ_r) and tangential (σ_θ) stresses can be written as:

$$\sigma_r = \left(1 - \frac{a^2}{r^2}\right) P_o + \left(\frac{a^2}{r^2}\right) P_i \qquad (24)$$

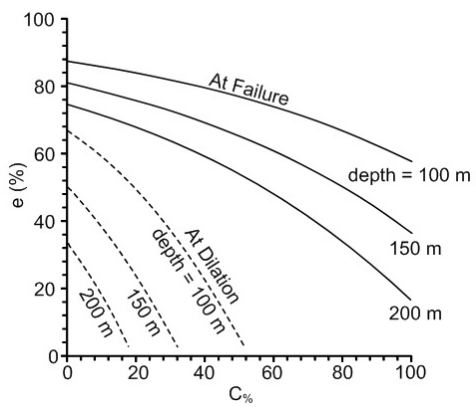

Figure 9. Extraction ratio as a function of the carnallite content ($C_{\%}$)

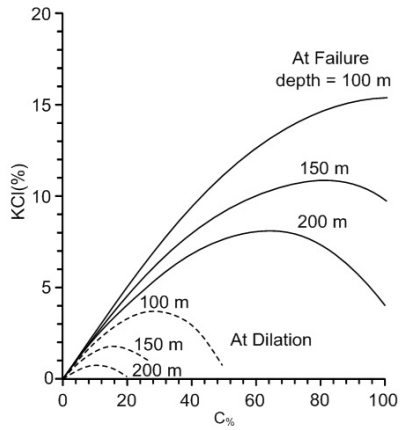

Figure 10. Weigh percent of sylvite (KCl) as a function of the $C_{\%}$ for various depths

$$\sigma_\theta = \left(1 + \frac{a^2}{r^2}\right) P_o - \left(\frac{a^2}{r^2}\right) P_i \qquad (25)$$

where a is the borehole radius, r is the radial distance from the center, and P_o and P_i are the constant external and internal pressures. Here P_i is assumed to be zero. Under the plane strain condition, the axial stress (σ_z) can be determined by:

$$\sigma_z = \nu\left(\sigma_r + \sigma_\theta\right) \qquad (26)$$

The surrounding salt is subjected to polyaxial compression, where the radial stress is the lowest, representing σ_3. The axial stress is σ_2, and the tangential stress is the greatest, representing σ_1. For this demonstration, P_o ranges from 5 and 10 to 15 MPa. They are equivalent to depths of approximately 200, 400, and 550 m, respectively. The FS at dilation and failure are defined as:

$$FS = \tau_{oct,d} / \tau_{oct} \qquad (27)$$

$$FS = \tau_{oct,f} / \tau_{oct} \qquad (28)$$

The zones of $FS \leq 1.0$ at dilation and failure around a borehole can be presented as a function of r/a for the various $C_{\%}$ values in Figure 11. The dilation and failure zones increase with the carnallite content and depths. These findings are useful for the selection of borehole casings and of sealing materials and methods after decommissioning.

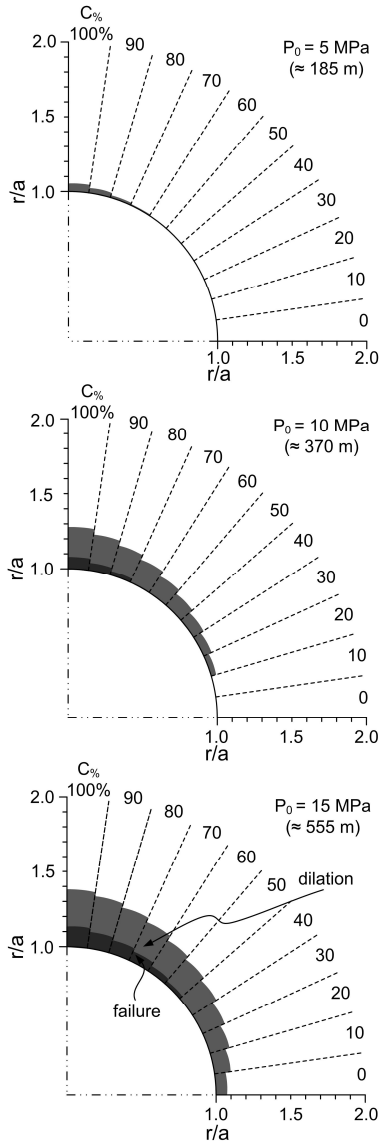

Figure 11. Zones of dilation and failure induced around boreholes penetrating through rock salt with the varying carnallite content and depths

Discussions and Conclusions

This study concentrates on the impact of the carnallite content on the mechanical properties of the specimens collected from the upper portion of the Lower Salt member. The specimens consist mainly of halite and carnallite, as evidenced by the XRD analyses performed in this study (Table 1). This supports the estimation method of the $C_{\%}$ for each specimen based on its density ratio (Equation 1) as being adequately reliable. The discrepancy between the carnallite content obtained by the chemical analyses and by the density ratio in Equation 1 may be caused by the preparation procedure to obtain the powder samples for the XRD analysis. Some hydroxyls may have been lost during grinding of the rock fragments.

The results clearly show that the $C_{\%}$ can significantly reduce the strengths and elastic moduli of the rock salt. The tensile strength can reduce to less than 0.5 MPa when the $C_{\%}$ approaches 100%. The uniaxial compressive

strengths of the pure carnallite are about 10 MPa or less than half of those of the pure halite. The strength conversion factors between the uniaxial compression test and the point load strength index decrease linearly from 13 for pure salt to 12 for pure carnallite. The elastic modulus rapidly decreases from about 17 GPa for pure halite to less than 2 GPa for the pure carnallite specimens. The increase of the Poisson's ratio as the $C_{\%}$ increases is supported by the fact that the halite crystals contain cleavages and intergranular boundaries that can be compressed under loading. The carnallite crystals, however, have no cleavage and are relatively soft. Thus, they are less compressible and tend to dilate more as compared with the halite crystals.

The Hoek-Brown criterion can adequately describe the strengths of the rock salt under varied amounts of the $C_{\%}$, both at dilation and at failure. The influence of the carnallite becomes smaller as the confining pressures increase. Sets of the empirical equations developed here can be used to determine the strengths and elasticity of the rock salt with varied amounts of the $C_{\%}$, which can be incorporated into the stability analysis and design of underground openings.

As demonstrated here, the proposed strength criterion as a function of the $C_{\%}$ can be applied to determine the appropriate extraction ratio of a potash mine and to predict the stability of exploratory boreholes that penetrate the salt and carnallite layers. Due to the low strength of the carnallite, the extraction ratio decreases with the increasing $C_{\%}$. The amount of the extracted sylvite can be optimized for any mine depth, as shown in Figure 10. Depending upon the time at which the backfill is installed, the pillar design from the dilation criterion can remain stable for longer than that from the failure criterion. The larger dilation zones induced around a borehole (Figure 11) suggest that the rate of borehole deformation (closure) will also be significant.

It should be noted that the test results obtained here are based on the rock salt specimens collected from 1 location and depth. They may not truly represent those of other mine locations and salt formations. Nevertheless, the effects of the $C_{\%}$ quantitatively determined here should be recognized and addressed for mine planning and stability assessment.

Acknowledgements

This study is funded by Suranaree University of Technology and by the Higher Education Promotion and National Research University of Thailand. Permission to publish this paper is gratefully acknowledged.

References

ASTM. (1998). D3967-08. Standard test method for splitting tensile strength of intact rock core specimens. ASTM International, West Conshohocken, PA, USA.

ASTM. (2007). D7012-07. Standard test method for compressive strength and elastic moduli of intact rock core specimens under varying states of stress and temperatures. ASTM International, West Conshohocken, PA, USA.

Biron, E. and Arioglu. E. (1980). Design of Supports in Mines. A Wiley Interscience Publicition, Istanbul, Turkey. 270p.

Brady, B.H.G. and Brown, E.T. (1985). Rock Mechanics for Underground Mining. 3rd ed. George Allen and Unwin, Australia. 571p.

Brown, E.T. (1981). Rock Characterization, Testing and Monitoring: ISRM Suggested Methods. 1st ed. Pergamon Press, Oxford, UK, 200p.

Crosby, K. (2005). An overview of geology and resources of the APPC Udon potash (sylvinite) deposits, Udon Thani province, Thailand. Proceedings of the International Conference on Geology, Geotechnology and Mineral Resources of Indochina; 28-30 November, 2005; Khon Kaen, Thailand, p. 1-10.

Franssen, R.C.M. and Spiers, C.J. (1990). Deformation of polycrystalline salt in compression and in shear at 250-350°C. In: Deformation Mechanisms, Rheology and Tectonics. Knipe, R.J. and Rutter, E.H., (eds). Geological Society, London, Special Publication, 45:201-213.

Fuenkajorn, K., Sriapai, T., and Samsri, P. (2012). Effects of loading rate on strength and deformability of Maha Sarakham salt. Eng. Geol., 135-136:10-23.

Fuenkajorn, K., Walsri. C., and Phueakphum, D. (2011). Intrinsic variability of the mechanical properties of Maha Sarakham salt. Q. J. Eng. Geol. Hydroge., 44:445-456.

Handin, J., Russell, J.E., and Carter, N.L. (1984). Transient creep of repository rocks, final report: Mechanistic creep laws for rock alts. National Technical Information Service, United States Department of Commerce, Springfield, VA, USA, 166p.

Hite, R.J. (1982). Progress report on the potash deposits of the Khorat Plateau, Thailand. U.S. Geological Survey, United States Department of the Interior, Reston, VA, USA, 70p.

Hite, R.J. and Japakasetr, T. (1979). Potash deposits of the Khorat Plateau, Thailand and Laos. Econ. Geol., 74(2):448-458.

Hoek, E. and Brown, E.T. (1980). Empirical strength criterion for rock masses. J. Geotech. Eng. ASCE, 160(GT9):1,013-1,035.

Jaeger, J.C., Cook, N.G.W. and Zimmerman, R.W. (2007). Fundamentals of Rock Mechanics Fourth Edition. Blackwell publishing, Oxford. 475p.

Klein, C., Hurlbut, C.S. and Dana, J.D. (1998). Manual of Mineralogy. John Wiley and Sons Inc. Wiley, New York. 571p.

Raj, S.V. and Pharr, G.M. (1992). Effect of temperature on the formation of creep substructure in sodium chloride single crystal. J. Am. Ceram. Soc., 75:347-352.

Senseny, P.E., Handin, J.W., Hansen, F.D. and Russell, J.E. (1992). Mechanical behavior of rock salt: phenomenology and micro-mechanisms. Int. J. Rock Mech. Min. 29:363-378.

Sriapai, T., Walsri, C. and Fuenkajorn, K. (2013). True-triaxial compressive strength of Maha Sarakham salt. Int. J. Rock Mech. Min., 61:256-265.

Suwanich, P. (1984). Potash and rock salt in Thailand. Proceedings of the Conference on the Geology and Mineral Resources of Thailand; 19-28 November, 1983; Bangkok, Thailand, p. 244-252.

Wisetsaen, S., Walsri, C. and Fuenkajorn, K. (2015). Effects of loading rate and temperature on tensile strength and deformation of rock salt. Int. J. Rock Mech. Min., 73:10-14.